ACCSCIENCE PUBLISHING

An International Journal of Optimization and Control: Theories & Applications
ISSN: 2146-0957 eISSN: 2146-5703
Vol.16, No.6, pp.2079-2098 (2026)
https://doi.org/10.36922/IJOCTA026160063

IJOCTA

RESEARCH ARTICLE

An efficient adaptive exponentially weighted moving average chart for effective fault detection in the process mean

Tahir Abbas[1]*, Hafiz Zafar Nazir[2], Muhammad Abid[3], and Muhammad Riaz[4]

[1]Department of Mathematics, College of Sciences, University of Sharjah, Sharjah, United Arab Emirates

[2]Department of Statistics, Faculty of Sciences, University of Sargodha, Sargodha, Punjab, Pakistan

[3]Department of Statistics, Faculty of Physical Science, Government College University Faisalabad, Faisala-bad, Punjab, Pakistan

[4]Department of Mathematics, College of Computing and Mathematics, King Fahd University of Petroleum and Minerals, Dhahran, Saudi Arabia

TAbbas@sharjah.ac.ae, zafar.nazir@uos.edu.pk, mabid@gcuf.edu.pk, riazm@kfupm.edu.sa

ARTICLE INFO

Article history:
Received: April 16, 2026
Revised: June 19, 2026
Accepted: June 23, 2026
Published online: November 13, 2026

Keywords:
Adaptive chart
Process monitoring
Monte Carlo simulations
Run length matrix
Statistical process control

ABSTRACT

The exponentially weighted moving average (EWMA) control charts with adaptive charting structures have attracted attention from the research community for their dynamically adjusted smoothing parameters, which improve sensitivity to both small and large process shifts. Unlike a traditional EWMA chart, it can maintain stability in normal conditions and detect deviations quickly, thereby improving monitoring efficiency. In this study, we propose a memory-based control chart for the monitoring of the process mean of a normally distributed process. It estimates the mean shifts with an EWMA-based estimator and then finds the smoothing constant for plotting the EWMA statistics using a proposed continuous function. Monte Carlo simulations are conducted to evaluate the performance of the proposed adaptive EWMA (AEWMA) chart under different shifts in the process mean. The run-length profiles metric, along with overall performance measures, was used as a performance evaluation tool, and the proposed AEWMA chart outperformed the competing methods. A real data set from a semiconductor manufacturing process, where the quality characteristic of interest is the wafer flow width, illustrates the applicability in practice.

CC BY

1. Introduction

Control charts are valuable tools for statistical process control because they are easy to use, very effective, and good at tracking changes in a process. It plays an important role in detecting special cause variations that can affect production, improve operational efficiency, and enhance product quality. Control charts are generally categorized into two types: memoryless and memory retentive. Memoryless charts use only the most recent data point to determine how to handle the process variables. They deliberately do not look at any past data points. If they used past data points, they might overreact to small changes in the process. Memory-based charts use past data, so they can detect subtle changes over the long term. That is why they are so valuable for securing long-term process stability and consistent quality control.[1]

Control charts are a vital tool of statistical process control to recognize when a process is out of control, so that adjustments can be made in time to maintain quality and efficiency.[2] Memory-based control charts, such as the cumulative sum (CUSUM)[3] and exponentially weighted moving average (EWMA)[4] charts, improve sensitivity by leveraging past data. The EWMA chart is highly effective at detecting small shifts and is more robust than Shewhart charts, especially

*Corresponding Author

in applications requiring tight control. These methods facilitate quick interventions, which are essential for advancing the quality and stability of processes across a wide range of industries. Further, these charts have been recently innovated and customized to detect specific types of changes and have been extensively discussed in[5] and.[6] Control charts are effective when the size of the shift is known as a priori or when the attention is focused on a small part of the process. However, their effectiveness is reduced if the shift size is unknown before monitoring.[7]

Researchers have proposed several adaptive procedures, such as the adaptive EWMA (AEWMA) chart.[8] It was proposed to use a comparative approach, tracking process performance using an AEWMA control chart. In the formation of the AEWMA chart, they used the Huber score function that can combine EWMA and Shewhart charts by modifying the weight of the previous data points depending on the magnitude of the observed error[9]:

$$e_t = y_t - x_{t-1} \tag{1}$$

This method allows the recognition of shifts of changing sizes while diminishing the effects of inertia, making it a more flexible and effective tool for quality control. Zhao *et al.*[10] applied the adaptive threshold method with EWMA to better monitor voltage changes in energy storage systems. Their method captures early evolving faults with a 99% or better cut-off for both false alarms and undetected faults. The method monotonically lessens the required man hours for system operation and inherent risk within the system. In the field of Bayesian process monitoring, Noor-ul-Amin and Noor[11] present an original AEWMA control chart that employs conjugate prior distributions to the squared-error and the linear-exponential loss functions to monitor changes in the process mean. The chart clearly outperformed the Bayesian EWMA control chart in an extensive comparison that used both Monte Carlo simulations and a real-life case study. The study by Sabahno *et al.*[12] suggests process monitoring techniques that simultaneously estimate both the mean vector and the covariance matrix of a multivariate normal quality characteristic. On the other hand, Noor-ul-Amin *et al.*[13] suggest a functional-based AEWMA multivariate control chart for monitoring the variance-covariance matrix of a normally distributed process. Computer simulations can be used to control the conditional false alarm probability, which in turn controls the conditional in-control average run length (ARL). The approach by Aytaçoğlu *et al.*[14] shows that these methods are viable for constructing AEWMA control charts where the smoothing parameter at each sampling instant depends on the value of the measured process quantity. Centofanti *et al.*[15] develop a basis denoted to as an adaptive multivariate functional control chart (AMFCC) that adapts the monitoring of a multivariate functional quality characteristic to an unknown out-of-control (OOC) distribution by combining p-values from partial tests, each of which is based on Hotelling's T^2-type statistics calculated for different parameter combinations.

Building on memory-based techniques, Haq *et al.*[16] developed the AEWMA chart based on an unbiased mean estimator. Their method showcases a bias-free estimator for detecting mean shifts. The authors suggest a step function, which defines the smoothing parameter of the EWMA statistic to be plotted on the control chart, which appears to be innovative. Moreover, it is worth noting that Sarwar and Noor-ul-Amin[17] proposed an AEWMA chart for the process mean monitoring in the case of a normally distributed process. The chart makes it possible to estimate the magnitude of the shift using the EWMA statistic, where the smoothing constant was chosen using a continuous function. The efficiency of the suggested method was proved for different magnitude shifts in the Monte Carlo experiments. Building upon this, we propose an enhanced AEWMA control chart for the process mean of a normally distributed controlled variable. Initially, the EWMA statistic is used with an estimator to detect mean shifts. Then, the smoothing parameter is estimated by applying a proposed continuous function, which is dependent upon the magnitude of the estimated shift. Next, the zero-state run-length distributions were generated using Monte Carlo simulations. The performance of the suggested control chart was assessed using average run length (ARL) and standard deviation of run length (SDRL) as elementary performance metrics. Moreover, the performance of the AEWMA charts was evaluated in terms of vibration monitoring quality.[18-20] It is important to note that the proposed control chart improves the ARL performance while also reducing false alarm rates. Indeed, during the implementation of control charts in practice, it is not always possible to specify the magnitude of process shifts; thus, it is relevant to assume that the shift size is a random variable, which should be estimated using an appropriate estimator.

The development of AEWMA control charts has evolved from discrete to continuous adaptation. The AEWMA-I chart suggested by Haq *et al.*[16] has a stepwise smoothing function that adapts to the shifts of the process mean in a piecewise manner. The adaptation in AEWMA-I corresponds to different regions of shift magnitude, with distinct smoothing parameter values. However, this adaptation can cause discontinuity in the sensitivity of the chart at the boundaries between adaptation regions. Sarwar and Noor-ul-Amin[17] proposed another AEWMA control chart (AEWMA-II) that uses a continuous function to capture abrupt changes in the process mean, without the discontinuity in adaptation found in AEWMA-I. However, it would be challenging to account for all the adaptation regions of shifts, in a continuous function, as different regions require different levels of sensitivity to detect shifts. Specifically, detecting smaller shifts requires higher sensitivity, whereas detecting larger shifts requires the fastest possible response. On the other hand, the AEWMA-III chart uses a six-segment adaptation scheme, with different functional forms used to detect small, moderate, and large shifts. Such an adaptation scheme can make the AEWMA-III chart more sensitive and flexible in responding to different levels of shifts. In the proposed AEWMA-III control chart, estimation of shifts is first made, and then, an innovative continuous adaptive function is introduced to estimate the smoothing parameter. The suggested innovation will enhance the chart's sensitivity while monitoring shifts of different magnitudes and, therefore, improve the chart's performance. The main objective of the proposed AEWMA-III chart is to develop a more flexible adaptive smoothing mechanism within the AEWMA framework. By employing multiple adaptation regimes, the proposed design provides smoother sensitivity transitions across different shift magnitudes and improves shift-detection performance while preserving the recursive structure and computational efficiency of existing AEWMA schemes.

The article is organized as follows: Section 2 presents detailed charting structures for the existing and proposed AEWMA control charts to examine a process's location parameter. Performance evaluation and comparative analysis are presented in Section 3. The application of the proposed chart in the manufacturing industry is described in Section 4. Section 5 presents the concluding remarks.

2. Existing and proposed structure of the AEWMA chart

This section presents the AEWMA charting structures of proposed and existing charts to monitor shifts in the process location of a normally distributed system. Let $\{Y_t\}$ represent a series of independent and identically distributed *(i.i.d.)* random variables, each following a normal distribution with mean θ and variance σ^2 at time $t \geq 1$. Initially, the process operates under in-control conditions for $t \leq t_0$. After this point $(t > t_0)$, an unknown shift in the mean occurs, moving the process into an OOC state, where the new mean is θ_1. In the OOC state, the distribution becomes:

$$X_t \sim N(\delta, 1) \ (i.e., \ Xt = \frac{(Yt - \theta)}{\sigma}) \tag{2}$$

with the shift size defined as:

$$\Upsilon = \frac{|\theta_1 - \theta|}{\sigma} \tag{3}$$

This standardization framework enables effective monitoring and detection of mean shifts in the process. In this context, t_0 and Υ denote the time of occurrence and the scale of the change, respectively, which are typically unknown. The primary goal of process monitoring is to identify the mean shift Υ as quickly as possible.

2.1. Design of the AEWMA-I control chart

This subsection presents the AEWMA-I chart designed by Haq *et al.*[16] to monitor shifts in the process location. The run-length descriptions of the proposed chart were evaluated using a Monte Carlo simulation. Let $\psi \in (0, 1]$ denote an additional smoothing constant; according to Jiang *et al.*,[21] an estimator for Υ is defined as:

$$\hat{\Upsilon}_t^* = \psi X_t + (1 - \psi)\hat{\Upsilon}_{t-1}^* \tag{4}$$

The preliminary estimate is set to $\hat{\Upsilon}_0^* = 0$. The estimator is unbiased under the in-control process situation, but exhibits bias out of sample. The unbiased estimator of Υ in both in-control and OOC situations is stated as follows:

$$\hat{\Upsilon}_t^{**} = \frac{\hat{\Upsilon}_t^{*}}{1-(1-\psi)^t} \tag{5}$$

For estimating Υ, it is suggested to utilize $\hat{\Upsilon}_t = \left|\Upsilon_t^{**}\right|$. The plotting statistic of the AEWMA-I chart, established on the sequence $\{X_t\}$ is defined as:

$$U_t = l\left(\hat{\Upsilon}_t\right)X_t + \left(1-l\left(\Upsilon_t\right)\right)U_{t-1} \tag{6}$$

where $U_0 = 0$ and $l\left(\hat{\Upsilon}_t\right) \in (0,1]$, such that:

$$l\left(\hat{\Upsilon}_t\right) = \begin{cases} 0.015 \ if \ 0.00 \le \hat{\Upsilon}_t \le 0.25 \\ 0.10 \ if \ 0.25 \le \hat{\Upsilon}_t \le 0.75 \\ 0.20 \ if \ 0.75 \le \hat{\Upsilon}_t \le 1.00 \\ 0.25 \ if \ 1.00 \le \Upsilon_t \le 1.50 \\ 0.50 \ if \ 1.50 \le \hat{\Upsilon}_t \le 2.50 \\ 0.80 \ if \ 2.50 \le \hat{\Upsilon}_t \le 3.50 \\ 1.00 \ if \ 3.50 < \hat{\Upsilon}_t \end{cases} \tag{7}$$

The proposed AEWMA chart generates an OOC signal whenever the statistic exceeds a specified threshold h.

2.2. Design of the AEWMA-II control chart

This subsection presents the AEWMA-II chart designed by Sarwar and Noor-ul-Amin[17] to monitor shifts in the process mean. This proposed chart uses the shift estimator δ and the unbiased estimator of Υ defined in **Equations 4 and 5**, respectively.

The AEWMA-II chart employs the following plotting statistic, which is computed from the sequence $\{X_t\}$.

$$V_t = g\left(\hat{\Upsilon}_t\right)X_t + \left(1-g\left(\hat{\Upsilon}_t\right)\right)V_{t-1} \tag{8}$$

where $V_0 = 0$ and $g\left(\hat{\Upsilon}_t\right) \in (0,1]$, such that:

$$g\left(\hat{\Upsilon}_t\right) = \begin{cases} \dfrac{1}{a\left[1+\left(\hat{\Upsilon}_t\right)^{-c}\right]} & if \ 0 < \hat{\Upsilon}_t \le 2.7 \\ 1 & if \ \hat{\Upsilon}_t > 2.7 \end{cases} \tag{9}$$

The constants a and c in **Equation 9** are assumed to be $a = 7$ and $c = 2$ when $\hat{\Upsilon}_t < 1$ and $c = 1$ when $1 < \hat{\Upsilon}_t \le 2.7$. These values are selected to ensure the proposed continuous function performs better in terms of ARL.

2.3. Design of the AEWMA-III control chart

This subsection presents the new AEWMA-III chart to monitor shifts in the process location. The run-length properties of the proposed chart were assessed using Monte Carlo simulations. The improved approach first applies to the EWMA statistic with an estimator to identify location shifts. Then, the smoothing parameter is calculated employing a newly introduced continuous function that alters based on the size of the estimated shift. This proposed chart uses the unbiased estimator of Υ defined in **Equations 4** and **5**, respectively. The AEWMA-III chart's plotting statistic, based on the sequence $\{X_t\}$, is defined as:

$$W_t = h\left(\hat{\Upsilon}_t\right)X_t + \left(1-h\left(\Upsilon_t\right)\right)W_{t-1} \tag{10}$$

where $W_0 = 0$ and $h\left(\hat{\Upsilon}_t\right) \in (0,1]$, such that:

$$h\left(\hat{\Upsilon}_t\right) = \begin{cases} \dfrac{\beta\hat{\Upsilon}_t^{\,2}}{\left[1+\left(\hat{\Upsilon}_t\right)^{-c}\right]} & if \ 0.0 \le \hat{\Upsilon}_t \le 1.0 \\ 0.015+(0.10-0.015).\dfrac{\hat{\Upsilon}_t}{0.25} & if \ 1.0 \le \hat{\Upsilon}_t \le 1.5 \\ 0.10+(0.30-0.10).log\left(1+\gamma\left(\hat{\Upsilon}_t-1.5\right)\right) & if \ 1.5 \le \Upsilon_t \le 2.7 \\ 1-\dfrac{exp\left(-k\left(\hat{\Upsilon}_t-d\right)\right)}{1+exp\left(-k\left(\hat{\Upsilon}_t-d\right)\right)} & if \ 2.7 \le \hat{\Upsilon}_t \le 3.5 \\ \dfrac{1}{1+exp\left(-2.5\left(\hat{\Upsilon}_t-3.5\right)\right)} & if \ 3.5 \le \hat{\Upsilon}_t \le 5.0 \\ 1.00 & if \ \hat{\Upsilon}_t > 5.0 \end{cases} \tag{11}$$

The proposed six-segment adaptive function was developed to ensure its ability to meet the different sensitivity requirements related to the process mean shifts of various sizes. Unlike the conventional approach, which relies on a single function, this approach uses multiple segments and their unique mathematical expressions to ensure a gradual response to minor shifts and greater sensitivity to large ones. In particular, the quadratic segment was adopted to ensure the function's stability and avoid extreme responses to very small shifts with changes in the process mean. Meanwhile, with linear and logarithmic segments, the increase in sensitivity to the changes in the process mean is gradual, and the utilization of logistic segments allows

for achieving a higher responsiveness to major process shifts and ensuring continuity. The values of $\beta = 0.05$, $\gamma = 1.2$, $k = 1.5$, and $d = 2.7$ were obtained through preliminary simulation studies and serve to balance the target in-control average run length and the required out-of-control performance.

The parameters of the continuous adaptation function given in **Equation 11** were chosen to address both minor and large process shifts appropriately. In particular, $a = 7$, $c = 2$ represent the scale and location factors, which determine the response level and starting point of the adaptation function. Particularly, $\beta = 0.05$ controls the chart's sensitivity to smaller process shifts. Given that, the smaller values of β result in a chart being insensitive to minor process shifts. On the other hand, the logistic growth parameter $\gamma = 1.2$ determines the extent to which the function grows on a logarithmic scale. Basically, a larger γ indicates a higher increase in the adaptation function. The logistic-growth parameters, $k = 1.5$, $d = 2.7$, also play a significant role in the adaptation function, where k represents the logistic growth's steepness while d determines the logistic growth's inflection point. Overall, with these parameters appropriately chosen, the function exhibits a moderate response to minor and moderate process shifts and a steeper response to large process shifts.

In terms of calculations, from a purely numerical point of view, the AEWMA-III chart proposed in this article leaves the recursive structure of AEWMA-I and AEWMA-II control charts intact. Therefore, for each sample, only three-stage calculations are required for the shift estimator Υ_t, the adaptive function, and the monitoring statistic W_t. This makes the memory requirements of the chart constant, as only the last values of Wt and Υ_t need to be stored for the computation of the next two statistics. Although it uses a piecewise continuous function that involves polynomial, logarithmic, and logistic terms, the chart only requires a constant number of arithmetic operations to calculate these expressions, which makes it asymptotically like the simpler AEWMA-I and AEWMA-II charts in terms of computational complexity. In fact, compared to AEWMA-I's stepwise function and AEWMA-II's continuous but nonlinear function, the three-stage calculation of AEWMA-III's monitoring statistic barely adds any additional computational burden. Therefore, the proposed AEWMA-III control chart can be easily used in practice for real-time monitoring and is significantly more powerful than its predecessors in detecting process shifts.

The proposed AEWMA-III plot was constructed using the unbiased shift estimator suggested by Haq *et al.*[16]; the rationale behind this choice was grounded in the successful application of this estimator in the previously developed AEWMA methodology and its use to estimate an updated shift magnitude. In this work, the unbiased shift estimator has not been modified; instead, a different smoothing function was designed to transform the estimated shift magnitude into an adaptive smoothing parameter. As such, the improved performance is primarily linked to the introduction of the new adaptive component. It must be stressed that in the current work, the finite-sample properties of the unbiased shift estimator were not evaluated, and the performance of the AEWMA chart was only investigated for independent observations. Therefore, future research will focus on assessing the performance of the procedure in the presence of autocorrelation. In addition, there is a need to explore alternative shift estimators and formalize theoretical properties regarding their applicability when combined with adaptive data-driven smoothing functions.

Decision rule: For the one-sided proposed AEWMA control chart, an out-of-control (OOC) signal is triggered whenever the statistic $|W_t|$ is greater than a certain threshold h. On the other hand, for the two-sided AEWMA control chart, the OOC signal is indicated if the statistic W_t is greater than h or smaller than -h. This means that it can identify deviation upward or downward in the process simultaneously. The threshold h is a positive number $(h > 0)$ that determines the value of ARL. The value of threshold h was selected separately for each value of ψ to achieve a desired in-control ARL (ARL_0).

3. Comparative analysis

The section delivers a thorough description and evaluation of how well the proposed and competing charts perform. Run-length characteristics were used to determine the performance of the existing AEWMA-I and AEWMA-II charts and the proposed chart AEWMA-III. In particular, the mean, standard deviation, and percentiles were employed as a primary run-length assessment tool for describing and comparing the performance of the competing and proposed charts. The comparison further evaluates the effectiveness of the proposed charts across a

range of shift values using overall performance measures: relative average run length (RARL), performance comparison index (PCI), and extra quadratic loss (EQL). Several approaches can be used to compute these run-length characteristics, including the probability method, Markov chain method, one-dimensional integral equation method, and Monte Carlo simulation.[22-30] For this study, we decided to use the Monte Carlo method because it is well established as a reliable approach for evaluating the performance of control charts. Using the Monte Carlo simulation, the run-length distributions for the proposed and existing charts were estimated by generating independent normal random samples with mean θ and unit variance. The mean shift parameter Υ was assigned specific values: 0.00, 0.25, 0.50, 0.75, 1.0, 1.5, 2.0, 2.5, 3.5, 4.0, 5.0, and 6.0, to thoroughly examine the chart's behavior under both in-control and OOC conditions. For the in-control ARL_0, target values of 200, 370, and 500 were chosen. In addition, the smoothing parameter was investigated for values of 0.10, 0.15, and 0.20 to identify the impact on the chart's performance. Moreover, these values of ψ were selected because they represent the most widely used values in the AEWMA literature, allowing for an objective comparison with existing control charts.

Therefore, as can be seen from the results presented in **Tables 1–4**, an extensive numerical experiment was carried out to evaluate the AEWMA-III control chart's performance in terms of ARL and SDRL for the zero-state process. Considering the findings, it is possible to conclude that the AEWMA-III chart outperforms all other charts for all levels of magnitude of shifts Υ in the process mean. Additionally, the chart's ability to detect both small and large shifts, as well as moderate ones, is higher than for the AEWMA-I and AEWMA-II charts. Moreover, its performance is the most consistent among the charts, as evidenced by the lowest ARL standard deviation. Specifically, the results of the AEWMA-III chart's performance are presented in **Tables 1–4**, whereas the comparison of the AEWMA-III, AEWMA-I, and AEWMA-II charts' performance is presented in **Tables 5** and **6**.

Tables 1–4 present the ARLs, SDRLs, and ARL percentiles of the proposed AEWMA-III control chart for different values of ARL_0, including 100, 370, and 500, with ψ = 0.15 and 0.2. Increasing the shift size Υ decreases the ARL_1 values. Specifically, for ARL_0 = 200, the AEWMA-III charts yielded ARL_1 values of 161.82, 53.74, 20.83, and 4.19 at Υ = 0.05, 0.20, 0.40, and 1.00, respectively. For ARL_0 = 370 and shifts of Υ = 0.05, 0.10, 0.15, and 0.20, the corresponding ARL_1s were 279.38, 74.62, 26.37, and 4.81. Similarly, at ARL_0 = 500, the chart achieved ARL_1s of 362.55, 86.07, 29.71, and 4.97 for Υ = 0.05, 0.20, 0.40, and 1.00, respectively. It is observed that there is a positive association between the ARL_1 values and ψ for the proposal chart. The increase in ψ from 0.15 to 0.20 also increased ARL_1 values and reduced the detection potential of the proposal chart; for example, when ψ = 0.15, ARL_0 = 500, and Υ = 0.10, ARL_1 was 209.71; with ψ = 0.20 and the same settings, ARL_1 was 292.45. This trend was observed across all shift levels, confirming the AEWMA-III chart's practicality for moderate and substantial shift sizes in process monitoring and quality control. The comparison results of the proposed AEWMA-III chart with the existing AEWMA-I and AEWMA-II charts are displayed in **Table 5** and **Table 6.** In **Table 5**, ARL and SDRL values of the AEWMA-III chart, and the other two AEWMA schemes at ψ = 0.10 and 0.15 for ARL_0 = 370 are presented. **Table 6** displays percentile matrices, and the AEWMA-III chart was superior to the AEWMA-I and AEWMA-II charts. For example, for ARL_0 = 370, when ψ = 0.15 and Υ = 0.20, the AEWMA-I produced ARL_1 = 89.85, AEWMA-II produced ARL_1 = 77.49, and AEWMA-III produced ARL_1 = 65.84. This implies that the AEWMA-III chart is indeed better than the competing chart in terms of fast detection of process faults. Similar results are expected for other shift sizes, noting that the reduction in ARL_1 values is higher for smaller shifts than for larger ones. On the other hand, the overall performance measures show similar conclusions as the AEWMA-III always has the lowest RARL, which means that its ARL is the closest to the best chart for all shifts, making it the better of the two charts. Thus, AEWMA-III has the lowest PCI, indicating better overall detection performance. AEWMA-III also has the lowest value of the EQL for both values of the smoothing parameter, which implies that it has the lowest weighted detection delay, especially for medium-large shifts. AEWMA-II comes second in all three performance criteria, while AEWMA-I has the highest RARL and EQL, meaning it has the worst overall detection performance. All three criteria used to evaluate the performance of AEWMA charts indicate that AEWMA-III is the best chart for use with ψ = 0.10 and ψ = 0.15 **(Table 5)**.

It is also noteworthy that the best performance of the proposed AEWMA-III chart is achieved for detecting small and moderate shifts, while all other charts practically immediately detect large shifts. It should be noted that although the improvement in terms of percentages may seem modest, the practical benefits in terms of reducing the production of defective items are significant for industrial processes. Finally, it is important to observe that the proposed AEWMA-III chart also preserves the recursive structure of the existing AEWMA charts, while at the same time achieving an improvement in detection power. Notably, the computational complexity per observation is no higher than that of the AEWMA schemes.

Table 1. Performance measures (ARL, SDRL, and run-length percentiles) of the proposed AEWMA-III control chart for $ARL_0 = 200$ and $\psi = 0.15$

Υ	ARL	SDRL	P_{05}	P_{10}	P_{25}	P_{50}	P_{75}	P_{90}	P_{95}
0.00	198.52	264.05	1	1	4	99.4	289	572	727
0.03	184.81	242.55	1	1	4	98	272	499	670
0.05	161.82	206.77	1	1	4	87	241	433	589
0.08	127.44	162.98	1	1	3	70	190	343	454
0.10	108.82	133.76	1	1	3	66	161	283	374
0.15	77.19	89.62	1	1	3	51	116	193	254
0.20	53.74	60.59	1	1	3	37	82	136	173
0.25	40.40	44.00	1	1	3	28	64	99	127
0.30	31.37	34.22	1	1	3	21	49	79	98
0.40	20.83	22.32	1	1	3	13	33	53	66
0.50	14.35	15.38	1	1	2	8	22	36	46
0.75	7.21	7.62	1	1	2	4	11	18	23
1.00	4.19	4.08	1	1	3	5	8	10	13
1.25	2.95	2.45	1	1	1	2	3	6	8
1.50	2.26	1.52	1	1	1	2	3	4	5
1.75	1.92	1.12	1	1	1	2	2	3	4
2.00	1.68	0.86	1	1	1	1	2	2	3
2.50	1.40	0.61	1	1	1	1	2	2	3
3.00	1.20	0.44	1	1	1	1	1	2	2
3.50	1.09	0.30	1	1	1	1	1	1	2
4.00	1.03	0.18	1	1	1	1	1	1	1
5.00	1.00	0.05	1	1	1	1	1	1	1
6.00	1.00	0.0	1	1	1	1	1	1	1

Table 2. Performance measures (ARL, SDRL, and run-length percentiles) of the proposed AEWMA-III control chart for ARL0 = 370 and $\psi = 0.15$

Υ	ARL	SDRL	P_{05}	P_{10}	P_{25}	P_{50}	P_{75}	P_{90}	P_{95}
0.00	370.89	466.56	1	2	11	209	511	970	1,136
0.03	317.54	417.52	1	2	8	183	476	876	1,071
0.05	279.38	347.93	1	2	7	162	402	727	985
0.08	208.85	249.35	1	2	7	130	311	536	717
0.10	166.49	198.91	1	2	6	105	244	427	565
0.15	106.82	119.96	1	2	5	73	160	263	352
0.20	74.62	78.72	1	2	5	56	114	189	227
0.25	53.14	54.62	1	2	4	40	83	127	160
0.30	41.10	42.11	1	2	4	31	65	97	123
0.40	26.37	27.05	1	2	3	18	42	64	79
0.50	18.04	18.90	1	2	3	11	28	45	56
0.75	8.32	8.69	1	1	2	4	12	21	26
1.00	4.81	4.67	1	1	2	3	6	12	15
1.25	3.21	2.56	1	1	2	2	4	6	8
1.50	2.54	1.64	1	1	1	2	3	4	6
1.75	2.13	1.19	1	1	1	2	3	4	4
2.00	1.86	0.93	1	1	1	2	2	3	4
2.50	1.51	0.69	1	1	1	1	2	2	3
3.00	1.27	0.51	1	1	1	1	2	2	2
3.50	1.12	0.34	1	1	1	1	1	2	2
4.00	1.05	0.22	1	1	1	1	1	1	2
5.00	1.00	0.06	1	1	1	1	1	1	1
6.00	1.00	0.06	1	1	1	1	1	1	1

Table 3. Performance measures (ARL, SDRL, and run-length percentiles) of the proposed AEWMA-III control chart for ARL0 = 500 and $\psi = 0.15$

Υ	ARL	SDRL	P_{05}	P_{10}	P_{25}	P_{50}	P_{75}	P_{90}	P_{95}
0.00	500.60	636.88	1	2	16	283	719	1,337	1,758
0.03	442.88	548.94	1	2	17	261	644	1,171	1,545
0.05	362.55	449.71	1	2	19	213	522	938	1,272
0.08	263.18	312.78	1	2	15	166	381	665	983
0.10	209.72	241.10	1	2	16	139	305	513	691
0.15	130.93	141.42	1	2	12	95	194	316	410
0.20	86.07	88.78	1	2	7	66	129	202	258
0.25	62.32	63.29	1	2	5	49	96	146	179
0.30	46.81	46.57	1	2	4	37	73	111	135
0.40	29.71	30.05	1	2	4	22	47	71	87

(*Cont'd...*)

Table 3. (*Continued*)

ϒ	ARL	SDRL	P_{05}	P_{10}	P_{25}	P_{50}	P_{75}	P_{90}	P_{95}
0.50	19.75	20.30	1	2	3	13	31	49	59
0.75	8.88	9.23	1	1	2	5	13	22	28
1.00	4.97	4.70	1	1	2	3	6	11	15
1.25	3.49	2.75	1	1	2	3	4	7	9
1.50	2.69	1.70	1	1	2	2	3	5	6
1.75	2.26	1.25	1	1	1	2	3	4	5
2.00	1.97	0.98	1	1	1	2	2	3	4
2.50	1.57	0.73	1	1	1	1	2	3	3
3.00	1.31	0.54	1	1	1	1	2	2	2
3.50	1.15	0.37	1	1	1	1	1	2	2
4.00	1.06	0.24	1	1	1	1	1	1	2
5.00	1.00	0.07	1	1	1	1	1	1	1
6.00	1.00	0.0	1	1	1	1	1	1	1

Table 4. Run-length profiles of the AEWMA-III control chart at ARL_0 of 200, 370, 500, and $\psi = 0.20$

ϒ	Threshold (h)					
	0.6303		0.7651		0.8503	
	ARL	SDRL	ARL	SDRL	ARL	SDRL
0.00	200.00	249.96	370.71	436.08	500.79	567.73
0.03	187.31	228.67	348.45	410.97	476.52	543.29
0.05	174.88	220.77	312.90	360.95	420.64	475.35
0.08	140.74	167.75	252.88	287.25	344.64	344.64
0.10	120.12	141.20	210.04	235.65	292.45	321.03
0.15	85.17	95.38	138.23	149.16	193.19	202.34
0.20	61.59	65.84	95.92	98.04	128.73	131.77
0.25	46.14	48.43	68.53	67.57	90.27	88.61
0.30	35.83	36.19	52.22	50.79	66.32	63.85
0.40	23.66	23.96	32.11	31.23	40.48	38.35
0.50	16.58	17.07	21.94	21.51	25.91	25.11
0.75	7.91	7.90	9.92	9.63	11.17	10.41
1.00	4.70	4.22	5.73	4.80	6.24	5.14
1.25	3.35	2.50	4.01	2.70	4.47	2.98
1.50	2.67	1.62	3.17	1.79	3.54	1.96
1.75	2.25	1.22	2.67	1.36	2.95	1.53
2.00	1.96	0.98	2.32	1.13	2.55	1.30
3.00	1.31	0.53	1.45	0.63	1.49	0.70
4.00	1.06	0.24	1.09	0.29	1.10	0.31
5.00	1.00	0.07	1.00	0.09	1.01	0.10

Table 5. Comparison of Proposed and Existing Charts based on run-length profiles for ARL0 = 370

Υ	$\Psi = 0.10$						$\Psi = 0.15$					
	AEWMA-I		**AEWMA-II**		**AEWMA-III**		**AEWMA-I**		**AEWMA-II**		**AEWMA-III**	
	$h = 0.8285$		$h = 0.4240$		$h = 0.5911$		$h = 0.9404$		$h = 0.4937$		$h = 0.4937$	
	ARL	**SDRL**	**ARL**	**SDRL**	**ARL**	**SDRL**	**ARL**	**SDRL**	**ARL**	**SDRL**	**ARL**	**SDRL**
0.00	371.14	463.75	369.10	406.79	370.88	495.92	370.90	434.82	370.46	366.37	370.89	466.56
0.03	342.64	421.34	329.63	351.53	318.54	448.90	351.09	410.76	334.89	327.70	317.54	417.52
0.05	312.72	382.02	281.71	292.40	267.85	364.03	319.02	374.60	287.61	276.52	279.38	347.93
0.08	240.65	293.25	202.86	198.74	192.97	245.46	264.36	307.33	216.96	199.21	208.85	249.35
0.10	202.78	245.80	168.25	159.15	151.73	193.99	227.34	262.07	179.09	159.15	166.49	198.91
0.15	133.91	156.48	109.67	99.25	94.17	111.03	153.46	175.30	117.33	95.66	106.82	119.96
0.20	89.85	102.51	77.49	66.94	65.84	74.90	105.51	118.64	83.02	63.40	74.62	78.72
0.25	66.13	73.76	56.71	48.19	48.38	54.14	74.57	82.65	62.34	45.36	53.14	54.62
0.30	48.74	55.69	43.93	35.99	35.57	40.10	55.32	60.16	49.07	34.78	41.10	42.11
0.40	30.40	34.36	28.15	23.40	22.50	25.38	32.96	35.17	32.69	22.48	26.37	27.05
0.50	19.49	22.02	19.69	16.12	15.22	17.55	21.54	22.51	23.47	15.80	18.04	18.90
0.75	8.63	9.24	9.74	7.44	7.16	7.92	9.56	9.35	12.34	7.87	8.32	8.69
1.00	4.73	4.52	6.02	4.24	4.11	4.17	5.40	4.89	7.86	4.66	4.81	4.67
1.25	3.15	2.70	4.26	2.69	2.84	2.45	3.59	3.01	5.57	3.04	3.21	2.56
1.50	2.33	1.82	3.25	1.86	2.23	1.66	2.61	2.07	4.25	2.20	2.54	1.64
1.75	1.85	1.29	2.65	1.37	1.82	1.09	2.02	1.47	3.39	1.73	2.13	1.19
2.00	1.56	0.99	2.22	1.07	1.62	0.83	1.66	1.09	2.79	1.42	1.86	0.93
2.50	1.21	0.56	1.71	0.73	1.33	0.57	1.27	0.61	2.00	1.03	1.51	0.69
3.00	1.07	0.30	1.41	0.55	1.17	0.40	1.10	0.34	1.52	0.74	1.27	0.51
3.50	1.02	0.16	1.20	0.41	1.07	0.27	1.03	0.19	1.24	0.50	1.12	0.34
4.00	1.00	0.07	1.09	0.29	1.02	0.16	1.01	0.10	1.10	0.32	1.05	0.22
5.00	1.00	0.01	1.00	0.09	1.00	0.04	1.00	0.02	1.01	0.10	1.00	0.06
6.00	1.00	0.00	1.00	0.00	1.00	0.00	1.00	0.00	1.00	0.02	1.00	0.06

Overall Performance Measures	**AEWMA-I**	**AEWMA-II**	**AEWMA-III**	**AEWMA-I**	**AEWMA-II**	**AEWMA-III**
	$\psi = 0.10$			$\psi = 0.15$		
RARL	1.1289	1.0792	1.0000	1.1652	1.0612	1.0000
PCI	1.1165	1.0143	1.0000	1.1120	1.0132	1.0000
EQL	2.2884	2.2374	2.0271	2.3485	2.1627	2.0212

Table 6. Comparison of run-length quantile profiles of the competing control charts for ARL0 = 370 with ψ = 0.15

Υ	Chart	ARL	SDRL	P_{05}	P_{10}	P_{25}	P_{50}	P_{75}	P_{90}	P_{95}
	AEWMA-I	370.90	434.82	1	2	49	229	533	937	1,237
0.00	AEWMA-II	370.46	366.37	17	40	110	260	514	848	1,102
	AEWMA-III	370.89	466.56	1	2	11	209	511	970	1,136
	AEWMA-I	351.45	414.03	1	2	47	216	506	886	1,185
0.03	AEWMA-II	334.89	327.70	16	37	101	236	464	761	987
	AEWMA-III	317.54	417.52	1	2	8	183	476	876	1,171
	AEWMA-I	320.56	373.27	1	2	45	199	461	810	1,072
0.05	AEWMA-II	287.61	276.52	15	35	91	206	397	647	840
	AEWMA-III	279.38	347.93	1	2	7	162	402	727	985
	AEWMA-I	264.10	306.43	1	2	38	164	378	667	884
0.08	AEWMA-II	216.96	199.21	14	31	76	160	298	474	611
	AEWMA-III	208.85	249.35	1	2	7	130	311	536	717
	AEWMA-I	228.17	265.24	1	2	33	142	329	575	762
0.10	AEWMA-II	179.09	159.15	13	27	67	136	244	387	493
	AEWMA-III	166.49	198.91	1	2	6	105	244	427	565
	AEWMA-I	154.52	175.95	1	1	24	99	222	383	504
0.15	AEWMA-II	117.33	95.66	11	21	49	94	159	243	304
	AEWMA-III	106.82	119.96	1	2	5	73	160	263	352
	AEWMA-I	105.11	118.30	1	1	16	69	151	259	342
0.20	AEWMA-II	83.02	63.40	9	17	37	69	113	166	205
	AEWMA-III	74.62	78.72	1	2	5	56	114	189	227
	AEWMA-I	75.12	83.29	1	1	12	50	108	184	241
0.25	AEWMA-II	62.34	45.36	8	13	29	53	85	122	150
	AEWMA-III	53.14	54.62	1	2	4	40	83	127	160
	AEWMA-I	55.72	60.70	1	1	10	37	81	135	176
0.30	AEWMA-II	49.07	34.78	7	11	23	42	67	95	116
	AEWMA-III	41.10	42.11	1	2	4	31	65	97	123
	AEWMA-I	33.03	35.29	1	1	7	22	48	79	103
0.40	AEWMA-II	32.69	22.48	5	8	15	28	45	63	75
	AEWMA-III	26.37	27.05	1	2	3	18	42	64	79
	AEWMA-I	21.55	22.52	1	1	5	15	31	51	66
0.50	AEWMA-II	23.47	15.80	4	6	11	20	32	45	54
	AEWMA-III	18.04	18.90	1	2	3	11	28	45	56
	AEWMA-I	9.53	9.30	1	1	2	7	13	22	28
0.75	AEWMA-II	12.34	7.87	3	4	6	11	16	23	28
	AEWMA-III	8.32	8.69	1	1	2	4	12	21	26

(*Cont'd...*)

Table 6. (*Continued*)

ϒ	Chart	ARL	SDRL	P_{05}	P_{10}	P_{25}	P_{50}	P_{75}	P_{90}	P_{95}
	AEWMA-I	5.43	4.87	1	1	1	4	8	12	15
1.00	AEWMA-II	7.86	4.66	2	3	5	7	10	14	17
	AEWMA-III	4.81	4.67	1	1	2	3	6	12	15
	AEWMA-I	3.58	3.01	1	1	1	3	5	8	9
1.25	AEWMA-II	5.57	3.04	1	2	4	5	7	10	11
	AEWMA-III	3.21	2.56	1	1	2	2	4	6	8
	AEWMA-I	2.62	2.08	1	1	1	2	4	5	7
1.50	AEWMA-II	4.25	2.20	1	1	3	4	5	7	8
	AEWMA-III	2.54	1.64	1	1	1	2	3	4	6
	AEWMA-I	2.02	1.48	1	1	1	1	3	4	5
1.75	AEWMA-II	3.39	1.73	1	1	2	3	4	6	6
	AEWMA-III	2.13	1.19	1	1	1	2	3	4	4
	AEWMA-I	1.66	1.09	1	1	1	1	2	3	4
2.00	AEWMA-II	2.79	1.42	1	1	2	3	4	5	5
	AEWMA-III	1.86	0.93	1	1	1	2	2	3	4
	AEWMA-I	1.26	0.60	1	1	1	1	1	2	2
2.50	AEWMA-II	2.00	1.03	1	1	1	2	3	3	4
	AEWMA-III	1.51	0.69	1	1	1	1	2	2	3
	AEWMA-I	1.10	0.34	1	1	1	1	1	1	2
3.00	AEWMA-II	1.52	0.74	1	1	1	1	2	3	3
	AEWMA-III	1.27	0.51	1	1	1	1	2	2	2
	AEWMA-I	1.03	0.19	1	1	1	1	1	1	1
3.50	AEWMA-II	1.24	0.50	1	1	1	1	1	2	2
	AEWMA-III	1.12	0.34	1	1	1	1	1	2	2

The present study primarily reported zero-state run-length performance, assuming the process shift occurred at the start of monitoring. Although this setting is useful for initial comparison, practical industrial shifts often occur after the chart has already reached its in-control operating regime. Therefore, steady-state performance is also important for assessing the effectiveness of real-time monitoring. In this context, a steady-state evaluation was conducted by allowing the chart to run under in-control conditions for a sufficiently long warm-up period (ξ = 100, 200), then introducing the process shift, provided no earlier false alarm occurred (**Table 7**). Moreover, relying solely on ARL may be insufficient, as the run-length distribution is often skewed. For this reason, SDRL and selected run-length percentiles (P_{25}, P_{50}, P_{75}) were also considered to provide a more complete description of chart performance. Then, the run length represents the OOC point, and the conditional expected delay at ξ can be expressed as:

$$D_{\xi} = E_{\xi}\left(RL - \xi + 1 | RL \geq \xi\right) \tag{12}$$

The proposed method is sensitive to the series of changes required to monitor the shift in the industrial process. The results show that when there was no process shift, the ARL values remained very close to the nominal ARL_0 = 200 for all alpha cuts, indicating that the chart maintained stable in-control performance under the steady-state condition. As the shift size increased, the ARL values decreased rapidly at ξ = 100 and 200, confirming the strong sensitivity of the proposed chart to detecting OOC

situations. For a shift of 0.03, the ARL values were found to be approximately 166, which implies that a small shift takes a relatively long time to detect. On the contrary, a shift of 0.10 and 0.20 had a significant decrease in ARL values to 63.50 and 37.70, respectively. This suggests that as the magnitude of the shift increases, the ARL decreases rapidly. For instance, ARL values for shift sizes of 3.00, 3.50, and above were approximately 1, which implies that large shifts can be detected almost immediately. It was also observed that as the shift size increased, the SDRL values decreased significantly, which indicates that the process of detecting large shifts is more consistent than detecting smaller shifts. Furthermore, it was noticed that all the ARL and SDRL values were almost constant for all alpha-cut levels. This shows that the proposed AEWMA-III chart was efficient, maintaining a desirable in-control ARL while exhibiting stable out-of-control ARL performance. Therefore, from these steady-state results, it was established that the proposed chart was effective in detection of all types of process shifts.

Table 7. Run-length profiles of the proposed AEWMA-III chart at $ARL_0 \approx 200$

Υ	$n = 5, \psi = 0.15, h = 0.2699, \xi = 100$					$n = 5, \psi = 0.15, h = 0.2694, \xi = 200$				
	ARL	**SDRL**	$\mathbf{P_{25}}$	$\mathbf{P_{50}}$	$\mathbf{P_{75}}$	**ARL**	**SDRL**	$\mathbf{P_{25}}$	$\mathbf{P_{50}}$	$\mathbf{P_{75}}$
0.00	199.15	194.52	60.00	139.00	280.00	199.75	194.21	61.00	141.00	276.25
0.03	166.27	162.84	50.00	116.00	233.00	163.97	164.71	49.00	115.00	224.00
0.05	124.21	116.92	41.00	89.00	171.00	123.60	114.66	41.00	89.00	172.00
0.08	83.82	74.55	32.00	62.00	114.00	83.91	72.26	31.00	62.00	112.00
0.10	63.50	54.07	25.00	49.00	85.00	62.72	53.20	25.75	49.00	86.00
0.15	37.70	29.25	17.00	30.00	50.00	37.75	28.19	18.00	31.00	50.00
0.20	25.87	17.61	13.00	22.00	34.00	25.80	17.28	13.00	22.00	34.00
0.25	19.36	12.14	11.00	17.00	25.00	19.09	11.85	11.00	17.00	25.00
0.30	15.25	9.13	9.00	14.00	20.00	15.24	9.10	9.00	14.00	20.00
0.40	10.62	5.77	6.00	10.00	14.00	10.55	5.62	7.00	10.00	14.00
0.50	7.96	3.99	5.00	7.00	10.00	7.96	4.03	5.00	7.00	10.00
0.75	4.89	2.22	3.00	5.00	6.00	4.93	2.22	3.00	5.00	6.00
1.00	3.54	1.48	2.00	3.00	4.00	3.55	1.49	2.00	3.00	4.00
1.25	2.79	1.13	2.00	3.00	4.00	2.78	1.14	2.00	3.00	3.00
1.50	2.32	0.90	2.00	2.00	3.00	2.30	0.90	2.00	2.00	3.00
1.75	1.98	0.76	1.00	2.00	2.00	1.97	0.76	1.00	2.00	2.00
2.00	1.74	0.66	1.00	2.00	2.00	1.73	0.66	1.00	2.00	2.00
2.50	1.42	0.52	1.00	1.00	2.00	1.41	0.52	1.00	1.00	2.00
3.00	1.19	0.40	1.00	1.00	1.00	1.20	0.40	1.00	1.00	1.00
3.50	1.07	0.25	1.00	1.00	1.00	1.07	0.25	1.00	1.00	1.00
4.00	1.02	0.13	1.00	1.00	1.00	1.02	0.13	1.00	1.00	1.00
5.00	1.00	0.01	1.00	1.00	1.00	1.00	0.00	1.00	1.00	1.00
6.00	1.00	0.00	1.00	1.00	1.00	1.00	0.00	1.00	1.00	1.00

The pictures below **(Figures 1** and **2)** show that the new AEWMA-III control chart has better performance than AEWMA-I and AEWMA-II control charts for small-to-moderate process shifts. The value of ARL computed for the proposed AEWMA-III control chart indicates that the process can detect shifts quickly. The use of the AEWMA-III control chart in a monitoring process helps reduce risks by detecting process changes early and taking corrective action. The proposed AEWMA-III control charts were found to be the best-performing control charts among the others based on the comparison results. It showed excellent performance, as evidenced by lower ARL and SDRL values. The AEWMA-III chart's high flexibility to handle different scenarios indicates that it can detect and monitor process changes effectively. In addition, sensitivity to small and moderate shifts can be achieved by setting a smaller value of ψ when a specific application needs high sensitivity to detect a minor process change.

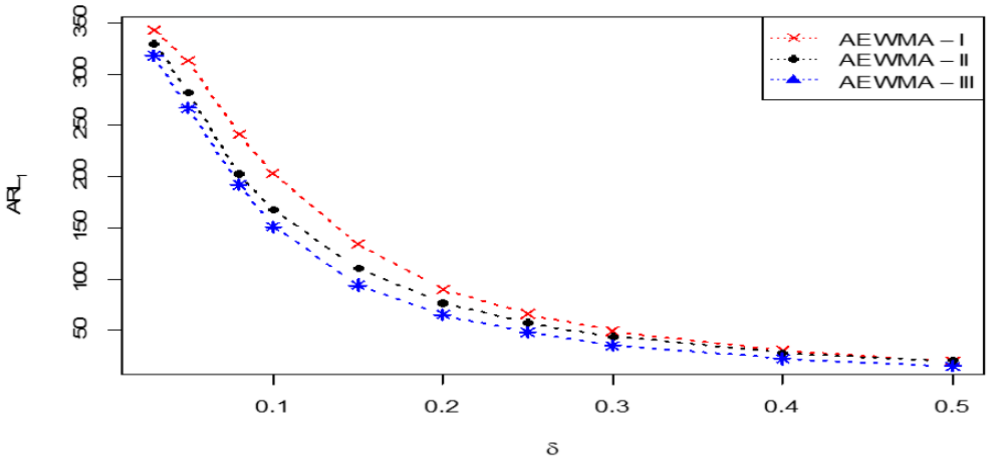


Figure 1. The ARL comparison for $\psi = 0.10$ and $ARL_0 = 370$

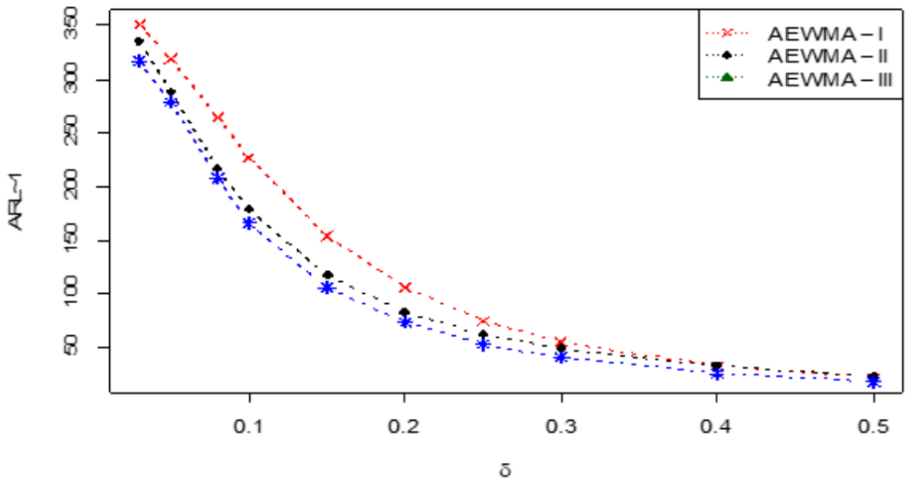


Figure 2. The ARL comparison for $\psi = 0.15$ and $ARL_0 = 370$

4. Illustrative example

In statistical process control, a common practice is to evaluate the performance of control charts through simulated and real-world data sets. Following this research tradition, in our study, we applied a real-world data set to illustrate the use and performance of AEWMA-II and the newly developed AEWMA-III control charts. As suggested by Montgomery,[31] we selected the data set from the semiconductor manufacturing industry, which consists of 45 samples, each including 5 wafers. The data set is related to the photolithography process followed by the post-exposure bake process, where the photoresist layer's flow width in microns was measured every hour.

The first thirty samples were from a process that was stable/in-control (Phase I) *($t_0 = 30$)*. The following fifteen samples were taken from the process with OOC (out-of-control) as shown by the figure below. A constant value of 0.017 was added to the observation to simulate an increase from the in-control process. The aim was to observe the process behavior and develop the control charts to detect an incipient change in the process.

Figures 3 and **4** demonstrate the performance of the two control charts under consideration during the surveillance period. For the first 30 samples, both the AEWMA-III and AEWMA-II schemes did not show any out-of-control (OOC) signals, suggesting that the process was under control. Nevertheless, for the last 15 samples, an upward shift of the process was detected by both charts, which implies a transition to the OOC state. It is also evident from the figures that the proposed AEWMA-III chart has a higher sensitivity to the OOC condition than the AEWMA-II scheme. While the AEWMA-III chart signals an OOC condition at the *35^{th}* sample, the AEWMA-II scheme responded only at the *43rd* sample. Therefore, the AEWMA-III control chart, which allows for a faster reaction to the OOC state, is more efficient for a faster reaction to the OOC state, is more efficient than the AEWMA-II alternative. Thus, the application of the AEWMA-III scheme to practice appears to be a viable option for most industries as it helps ensure high-quality products by quickly detecting small process shifts.

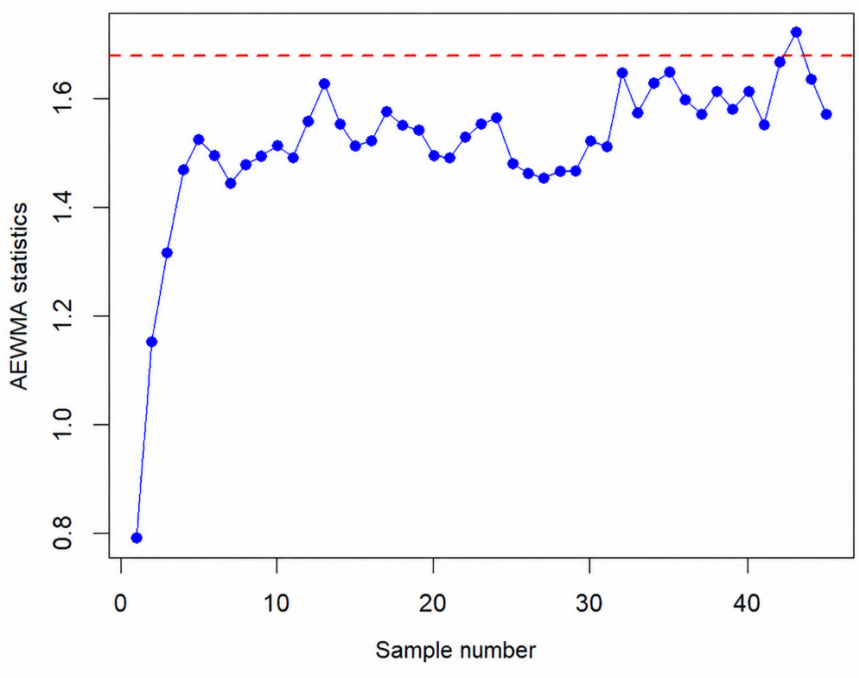


Figure 3. The flow width of the AEWMA-II control chart

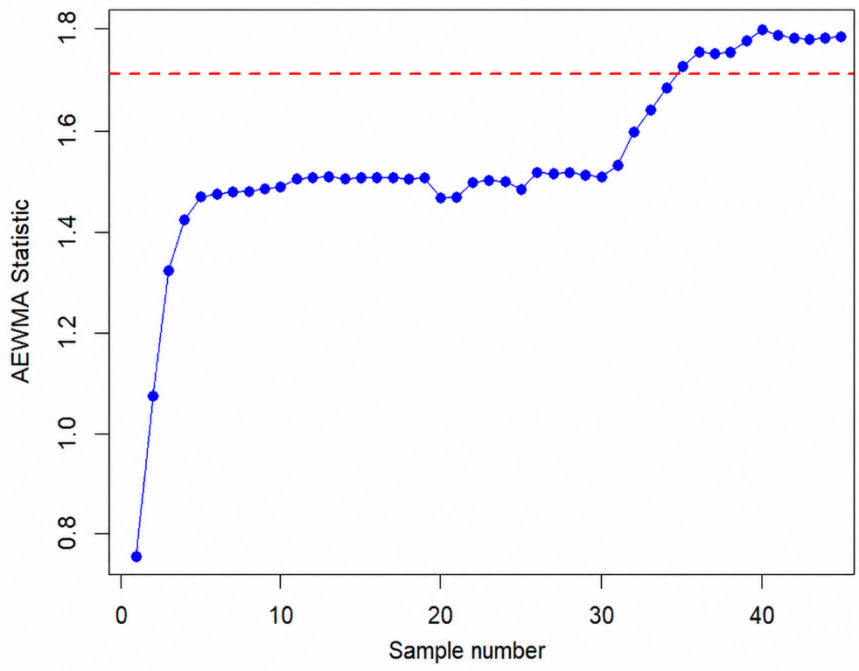


Figure 4. The flow width of the proposed AEWMA-III control chart

5. Conclusion

The paper introduces an innovative AEWMA-III control chart, which improves the performance of detecting mean shifts in the process. The new procedure uses a memory-type EWMA estimator with a varying smoothing constant to efficiently respond to both small and large shifts in the process parameter. Extensive simulations demonstrate the effectiveness of the proposed method, as the AEWMA-III chart has better run-length properties than existing procedures. The AEWMA-III chart performs consistently well and maintains a stable in-control state when no process shifts are present. However, it rapidly detects small and moderate process shifts after their occurrence. The comparison shows that while AEWMA-I, AEWMA-II, and EWMA charts exhibit similar performance in detecting large process shifts (almost immediate detection), AEWMA-III demonstrates overall superiority. Although the improvements in terms of percentage might seem insignificant for specific process shifts, in practice, even small changes in the early stages of a shift can lead to a substantial reduction in the number of nonconforming items produced. However, one disadvantage of the proposed procedure is that it primarily focuses on detecting small and moderate shifts. The other methods perform comparably when detecting large shifts. At the same time, the AEWMA-III chart can still be used for processes with large shifts as it efficiently tracks both small and large shifts. The proposed chart, however, is more effective in detecting small and moderate shifts. In most cases, such shifts do not become apparent at the initial stage of the process. Thus, the ability to quickly detect such shifts after they occur is particularly important for any production process. The AEWMA-III chart can help producers maintain high-quality production by reducing the likelihood of large numbers of nonconforming items. Such items can be detected and eliminated from the production process early, thereby reducing losses and costs. Finally, the new chart efficiently integrates with the previously used recursive procedures to monitor process shifts, enabling calculations for each observation without significantly increasing complexity. The effectiveness and performance of the proposed approach were verified as an example of a semiconductor manufacturing process. The analysis of actual wafer width flow data shows that using the AEWMA-III chart enables efficient process monitoring.

Finally, we can say that the newly designed AEWMA-III control chart is beneficial for statistical process control in terms of theory and practice. Moreover, the proposed AEWMA-III control chart is highly flexible and sensitive. Therefore, it has great potential to be widely

applied in modern industrial quality control processes. In addition, it also has the potential to be further developed into AEWMA control charts for detecting shifts in variance or simultaneously detecting shifts in both the process mean and variance. On the other hand, the proposed AEWMA-III control chart also has some shortcomings. As mentioned above, the proposed control chart was designed and investigated only for normal observations and independent process data. Therefore, there are still many practical problems to be solved, such as the performance of the proposed AEWMA-III control chart when observations come from other distributions or when the data are dependent (autocorrelated). However, the proposed adaptive method is also very flexible and has very good potential for further development. In our future work, we can further develop non-random AEWMA-III control charts for detecting process shifts in non-normal processes. Another direction for future research is to study how to apply the newly designed AEWMA-III control chart to autocorrelated process data, which is also very common in industrial processes. At the same time, it is also of great significance and value to extend the newly designed AEWMA-III control chart to the multivariate case, to enable AEWMA control charts to be widely used in the field of industrial statistics.

Acknowledgments

The author, Tahir Abbas, is grateful to the Office of the Vice Chancellor for Research and Graduate Studies (VCRG) at the University of Sharjah, United Arab Emirates, for excellent research facilities.

Funding

This work was supported by the Office of the Vice Chancellor for Research and Graduate Studies (VCRG) at the University of Sharjah, United Arab Emirates, under Project 24021440167.

Conflict of interest

The author declares no conflicts of interest that could have influenced the work reported in this paper.

Author contributions

Conceptualization: Tahir Abbas, Hafiz Zafar Nazir
Formal analysis: Tahir Abbas
Investigation: Tahir Abbas, Muhammad Abid
Methodology: Tahir Abbas
Supervision: Muhammad Riaz
Writing–original draft: Tahir Abbas
Writing–review & editing: All authors

Availability of data

The data are available from the corresponding author upon reasonable request.

AI tools statement

All authors confirm that no AI tools were used in the preparation of this manuscript.

References

1. Baranwal A, Kumar N, Chatterjee K, Koukouvinos C. A new EWMA chart for simultaneously monitoring the parameters of a shifted exponential distribution. *J Appl Stat.* 2025;52(1):221-252. https://doi.org/10.1080/02664763.2024.2363404
2. Hayter AJ, Tsui K-L. Identification and quantification in multivariate quality control problems. *J Qual Technol.* 1994;26(3):197-208. https://doi.org/10.1080/00224065.1994.11979526
3. Page E. Cumulative sum charts. *Technometrics.* 1961;3(1):1-9. https://doi.org/10.1080/00401706.1961.10489922
4. Roberts S. Control chart tests based on geometric moving averages. *Technometrics.* 1959;1(3):239-250. https://doi.org/10.1080/00401706.2000.10485986
5. Noor-ul-Amin M, Javaid A, Hanif M, Dogu E. Performance of maximum EWMA control chart in the presence of measurement error using auxiliary information. *Commun Stat-Simul Comput.* 2022;51(9):5482-5506. https://doi.org/10.1080/03610918.2020.1772301
6. Riaz M, Abbas Z, Nazir HZ, Akhtar N, Abid M. On designing a progressive EWMA structure for an efficient monitoring of silicate enactment in hard bake processes. *Arab J Sci Eng.* 2021;46:1743-1760. https://doi.org/10.1007/s13369-020-04948-y
7. Rasheed Z, Khan M, Anwar SM, Aslam MU, Lone SA, Almutlak SA. Designing an efficient adaptive EWMA model for normal process with engineering applications. *Ain Shams Eng J.* 2024:102904. https://doi.org/10.1016/j.asej.2024.102904
8. Capizzi G, Masarotto G. An adaptive exponentially weighted moving average control chart. *Technometrics.* 2003;45(3):199-207. https://doi.org/10.1198/004017003000000023
9. Ahmadini AA, Abbas T, AlQadi H. Adaptive EWMA Control Chart by Adjusting the Risk

Factors through Artificial Neural Network. *Qual Reliab Eng Int.* 2025;41(3):992-1001. https://doi.org/10.1002/qre.3696
10. Zhao J, Gao L, Huang B, *et al.* Dynamic monitoring of voltage difference fault in energy storage system based on adaptive threshold algorithm. IEEE; 2020:2413-2418. https://doi.org/10.1109/EI250167.2020.9347044
11. Noor-ul-Amin M, Noor S. An adaptive EWMA control chart for monitoring the process mean in Bayesian theory under different loss functions. *Qual Reliab Eng Int.* 2021;37(2):804-819. https://doi.org/10.1002/qre.2764
12. Sabahno H, Amiri A, Castagliola P. A new adaptive control chart for the simultaneous monitoring of the mean and variability of multivariate normal processes. *Comput Ind Eng.* 2021;151:106524. https://doi.org/10.1016/j.cie.2020.106524
13. Noor-ul-Amin M, Sarwar MA, Emam W, Tashkandy Y, Yasmeen U, Nabi M. Adaptive multivariate dispersion control chart with application to bimetal thermostat data. *Sci Rep.* 2023;13(1):18137. https://doi.org/10.1038/s41598-023-45399-3
14. Aytaçoğlu B, Driscoll AR, Woodall WH. Design of adaptive EWMA control charts using the conditional false alarm rate. *Qual Reliab Eng Int.* 2023;39(6):2206-2214. https://doi.org/10.1002/qre.3324
15. Centofanti F, Lepore A, Palumbo B. An Adaptive Multivariate Functional Control Chart. *Technometrics.* 2025;67(4):603-616. https://doi.org/10.1080/00401706.2025.2491369
16. Haq A, Gulzar R, Khoo MB. An efficient adaptive EWMA control chart for monitoring the process mean. *Qual Reliab Eng Int.* 2018;34(4):563-571. https://doi.org/10.1002/qre.2272
17. Sarwar MA, Noor-ul-Amin M. Design of a new adaptive EWMA control chart. *Qual Reliab Eng Int.* 2022;38(7):3422-3436. https://doi.org/10.1002/qre.3141
18. Zaagan AA, Khan I, Alzahrani ARR, Ahmad B. Parameter free AEWMA control chart for dispersion in semiconductor manufacturing. *Sci Rep.* 2024;14(1):10512. https://doi.org/10.1038/s41598-024-61408-5
19. Naveed M, Azam M, Khan N, Aslam M, Saleem M, Saeed M. Control chart for half normal and half exponential power distributed process. *Sci Rep.* 2023/05/27 2023;13(1):8632. https://doi.org/10.1038/s41598-023-35884-0
20. Jones CL, Abdel-Salam ASG, Mays DA. Novel Bayesian CUSUM and EWMA control charts via various loss functions for monitoring processes. *Qual Reliab Eng Int.* 2023;39(1):164-189. https://doi.org/10.1002/qre.3229
21. Jiang W, Shu L, Apley DW. Adaptive CUSUM procedures with EWMA-based shift estimators. *Iie Trans.* 2008;40(10):992-1003. https://doi.org/10.1080/07408170801961412
22. Abbas T, Riaz M, Javed B, Abujiya MaR. A new scheme of dispersion charts based on neoteric ranked set sampling. *AIMS Math.* 2023;8(8):17996-18020. https://doi:10.3934/math.2023915
23. Erto P, Pallotta G, Mastrangelo CM. A semi-empirical Bayesian chart to monitor Weibull percentiles. *Scand J Stat.* 2015;42(3):701-712. https://doi.org/10.1111/sjos.12131
24. Gandy A, Kvaløy JT. Guaranteed conditional performance of control charts via bootstrap methods. *Scand J Stat.* 2013;40(4):647-668. https://doi.org/10.1002/sjos.12006
25. Centofanti F. Statistical Process Monitoring Based on Functional Data Analysis. *Wiley Interdiscip Rev Comput Stat.* 2026;18(1):e70057. https://doi.org/10.1002/wics.70057
26. Grimm TR, Newhart KB, Hering AS. Nonparametric Threshold Estimation of Autocorrelated Statistics in Multivariate Statistical Process Monitoring. *J Chemom.* 2025;39(2):e70004. https://doi.org/10.1002/cem.70004
27. Abbas T, Nazir HZ, Husssain Z, Abbas Z, Akhtar N. An Adaptive EWMA Dispersion Control Chart Basedon Robust Estimators Under Ranked Set Sampling. *J Prime Res Math.* 2026:11-27. https://jprm.sms.edu.pk/index.php/jprm/article/view/580
28. Toktaş P, Gebizlioğlu ÖL. Modeling the dependency structure between quality characteristics in multi-stage manufacturing processes with copula functions. *Int J Optim Control Theor Appl.* 2024;14(4):404. https://doi.org/10.11121/ijocta.1594
29. Anwar SM, Almakayeel N, Lin C-Y. Efficient monitoring of exponential processes using memory control charts for healthcare applications. *Sci Rep.* 2026. https://doi.org/10.1038/s41598-026-47544-0
30. Bayati M, Nasrollahzadeh S, Bameni Moghadam M. Robust Monitoring of Multivariate Location Using a New Nonparametric Depth-Based Control Chart. *J Appl Math.* 2026;2026(1):2550562. https://doi.org/10.1155/jama/2550562
31. Montgomery DC. *Introduction to statistical quality control.* John wiley & sons; 2019.

Tahir Abbas *acquired his M.Sc. and M.Phil. degrees in Statistics from Quaid-i-Azam University, Islamabad, Pakistan, in 2006 and 2010. He earned his Ph.D. degree in Statistics from Xiamen University, Xiamen, China, in 2016. He was a lecturer in the Department of Statistics, Government College University, Lahore 54000, Pakistan, from 2012 to 2017 and an Assistant Professor from 2017 to 2022. Currently, he is working as an Associate Professor at the University of Sharjah, Sharjah, UAE. His current research interests include Statistical Process Control (SPC) and linear profile monitoring, Econometrics, and Bayesian Statistics.*

https://orcid.org/0000-0001-5208-5374

Hafiz Zafar Nazir *obtained his MSc and MPhil degrees in statistics from the Department of Statistics, Quaid-i-Azam University, Islamabad, Pakistan, in 2006 and 2008, respectively. He did his Ph.D. in statistics from the Institute of Business and Industrial Statistics, University of Amsterdam, The Netherlands, in 2014. Currently, He is serving as an Associate Professor in the Department of Statistics at the University of Sargodha, Pakistan. His current research interests include statistical process control, non-parametric techniques, and robust methods.*
https://orcid.org/0000-0003-2073-918X

Muhammad Abid *is working as an Associate Professor in the Department of Statistics at Government College University Faisalabad, Pakistan. He received his M.Phil. and M.Sc. in Statistics from Quaid-i-Azam University, Islamabad, Pakistan, in 2008 and 2010; he received his Ph.D. in Statistics from Zhejiang University, Hangzhou, China. His research interests include SPC, Nonparametric, Computational, and Bayesian Statistics.*
https://orcid.org/0000-0001-9998-9960

Muhammad Riaz *earned a Ph.D. in Statistics from the Institute of Business and Industrial Statistics, University of Amsterdam, The Netherlands, in 2008. He is serving as a Professor in the Department of Mathematics at King Fahd University of Petroleum and Minerals, Dhahran 31261, Saudi Arabia. His current research interests include Statistical Process Control, Non-Parametric Techniques, Experimental Designs, and Computational Statistics (focusing on Code Development).*
https://orcid.org/0000-0002-7599-6928

An International Journal of Optimization and Control: Theories & Applications (https://accscience.com/journal/ijocta)



This work is licensed under a Creative Commons Attribution 4.0 International License. The authors retain ownership of the copyright for their article, but they allow anyone to download, reuse, reprint, modify, distribute, and/or copy articles in IJOCTA, so long as the original authors and source are credited. To see the complete license contents, please visit http://creativecommons.org/licenses/by/4.0/.